

Optomechanical laser cooling with mechanical modulations

Marc Bienert

Theoretische Physik, Universität des Saarlandes, D-66123 Saarbrücken, Germany

Pablo Barberis-Blostein

*Instituto de Investigaciones en Matemáticas Aplicadas y en Sistemas,
Universidad Nacional Autónoma de México, Circuito Escolar s/n Ciudad Universitaria México, D.F.*

(Dated: April 16, 2018)

We theoretically study the laser cooling of cavity optomechanics when the mechanical resonance frequency and damping depend on time. In the regime of weak optomechanical coupling we extend the theory of laser cooling using an adiabatic approximation. We discuss the modifications of the cooling dynamics and compare it with numerical simulations in a wide range of modulation frequencies.

I. INTRODUCTION

Quantum cavity optomechanics [1] deals with the physics of a mechanical element coupled to the light field of an optical resonator by radiation forces in the quantum regime. In the simplest and most commonly used model a single mechanical harmonic oscillator is coupled to a single mode of an optical cavity by radiation pressure interaction being proportional to the light intensity. The prototype of an optomechanical setup is a Fabry-Perot cavity with pendular end-mirror, whose microfabricated realization [2], but also other implementations [3–6], have been developed in the laboratories worldwide. The optomechanical coupling allows for optical control of the mechanical object, manifesting itself in strongly modified mechanical properties what ultimately can lead to laser cooling [7–9] towards the mechanical ground state, as has been demonstrated in a certain setup [10], marking a requisite milestone on the way to quantum applications.

For typical realizations, the optomechanical coupling is clearly smaller than the mechanical frequency. In such a regime, laser cooling can be considered as a consequence of Raman scattering of photons with Stokes- and anti-Stokes events, where a single vibrational quantum is deposited or taken away with the scattered photon. These processes play the central role in the cooling dynamics, similar as in the Lamb-Dicke regime of laser cooling of atoms. When Anti-Stokes scattering prevails, the mechanical system is cooled. The balance between Stokes- and Anti-Stokes scattering can be adjusted by the laser parameters and for resolved sideband cooling, when the cavity's linewidth is smaller than the mechanical frequency ν , the pump laser optimally has to be detuned to the red side of the cavity resonance by ν .

The optomechanical coupling strength is typically even so weak, that cooling with single photons turns out to be much too slow to overcome the rethermalization rate due to the coupling with the mechanical element's environment at cryogenic or even room temperature. To overcome this obstacle, in many setups a strong pump laser is used to effectively boost the optomechanical interaction. Beyond that, more sophisticated cooling schemes

are based on pulsed pump schemes exploiting interference effects [11, 12], or dynamically controlled cavity dissipation [13] in order to improve the cooling efficiency. Short optical pulses can also be used for state preparation and reconstruction [14], and modulated driving allows for the generation of squeezed quantum states [15]. The modulation of the mechanical frequency was investigated in Ref. [16] with the result that squeezing and entanglement are enhanced in a resonant manner when the modulation frequency is twice the mechanical frequency, while the mean vibrational occupation number is simultaneously increased.

In this work, we focus on the behavior of laser cooling when the mechanical frequency and the mechanical damping is varied in time. This investigation was motivated by the recent experimental work [17] using dielectric membranes oscillatingly mounted inside a Fabry-Perot cavity. By local heating of the membrane with the help of a laser beam, both the resonance frequency of a vibrational mode and the linewidth can be altered in a controlled way. We extend the theory of optomechanical cooling to include modulations of the mechanical frequency in an adiabatic way and compare the predictions with numerical results. Moreover, we discuss how the modulated damping rates influences the cooling behaviour. We find that in the resolved sideband limit and for strong periodic modulations, additional cooling resonances appear. For weaker modulations or larger cavity linewidths these resonances overlap and with the help of different pulse shapes, the form of the resulting resonances can be influenced. Moreover, we systematically scan a large range of modulation parameters and discuss the cooling behavior in the various regimes.

This article is set up as follows: We first provide a theoretical description of the model in Sec. II by presenting the master equation of the open quantum system and the linearized model used for numerical calculations. In Sec. III we extend the theory of optomechanical cooling by including the temporal changes of the mechanical frequency into the description using an adiabatic approximation. Moreover, we point out the changes due to the modulation and compare them with numerical calculations. In Sec. IV, we then focus on a larger range of mod-

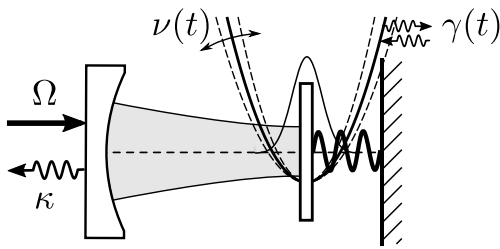


FIG. 1. An optomechanical setup, consisting of an optical cavity coupled to a harmonically supported mechanical element by radiation forces, experiences modulations of the mechanical properties, *i.e.* periodically changes in the mechanical frequency $\nu(t)$ and damping rate $\gamma(t)$. The cavity is pumped by an external laser at rate Ω while photons leak out of the cavity at rate 2κ . For certain parameters, the light scattering leads to cooling of the mechanical motion, which is influenced by the mechanical modulation.

ulation frequencies and damping rates of the mechanical oscillator. We discuss the numerical findings and connect them to the theory of modulated cooling. Finally, in Sec. V, we summarize and draw the conclusions.

II. MODULATED OPTOMECHANICAL SETUP

A. Model

We consider an optomechanical setup consisting of a single mechanical oscillator of effective mass M coupled by radiation forces to a single driven mode of an optical cavity with frequency ω_{cav} , see Fig. 1. The Hamiltonian for such a setup in the frame rotating with the frequency ω_{p} of the pump laser reads

$$H(t) = H_{\text{cav}} + H_{\text{mec}}(t) + H_{\text{rad}} + W \quad (1)$$

whereby

$$H_{\text{cav}} = -\hbar\delta a^\dagger a \quad (2)$$

$$H_{\text{mec}}(t) = \frac{p^2}{2M} + \frac{1}{2}M\nu(t)^2 x^2 \quad (3)$$

are the unperturbed Hamiltonians of the cavity mode with detuning $\delta = \omega_{\text{pump}} - \omega_{\text{cav}}$ and the mechanical oscillator with time-dependent frequency $\nu(t)$, respectively. The annihilation operator a of a single photon in the cavity obey $[a, a^\dagger] = 1$. The mechanical oscillator's position and momentum operators x and p are connected to the time-independent annihilation operator by

$$b_0 = \frac{1}{2\xi_0}x + i\frac{\xi_0}{\hbar}p \quad (4)$$

where we introduced the harmonic oscillator's length scale

$$\xi_0 = \sqrt{\frac{\hbar}{2M\nu_0}}, \quad (5)$$

with the time-averaged oscillator frequency $\nu_0 = \frac{1}{T} \int_0^T \nu(t) dt$ over one period T of the modulation. The optical and mechanical degree of freedom is coupled by radiation forces of the form

$$\begin{aligned} H_{\text{rad}} &= -\hbar g a^\dagger a x \\ &= -\hbar\chi_0 a^\dagger a [b_0 + b_0^\dagger]. \end{aligned} \quad (6)$$

Here, $\hbar\chi_0/\xi_0 = \hbar g$ can be interpreted as the time-independent radiation force a single photon exerts on the unmodulated mechanical oscillator. In a Fabry-Perot setup like in Fig. 1, $\chi_0 = \omega_{\text{c}} \xi_0/L$, where L denotes the static cavity length. For the membrane in the middle setup, an additional factor including the membranes electric field reflectivity and its position within the unperturbed mode function of the cavity has to be included [18, 19]. The pump of the cavity is taken into account by

$$W = \hbar\frac{\Omega}{2}(a + a^\dagger). \quad (7)$$

With the Hamiltonian H , Eq. (1), we can write down the master equation

$$\frac{\partial \rho}{\partial t} = \frac{1}{i\hbar}[H(t), \rho] + \mathcal{L}_\kappa \rho + \mathcal{L}_\gamma(t) \rho \quad (8)$$

where

$$\begin{aligned} \mathcal{L}_\kappa \rho &= \kappa \mathcal{D}[a] \rho \\ &= \kappa \mathcal{D}[a] \rho \end{aligned} \quad (9)$$

$$(10)$$

describe cavity losses with decay rate κ . The damping of the oscillator with a time dependent damping rate $\gamma(t)$ we approximately describe by

$$\mathcal{L}_\gamma(t) \rho = \frac{\gamma(t)}{2}(\bar{m} + 1)\mathcal{D}[b_0] \rho + \frac{\gamma(t)}{2}\bar{m}\mathcal{D}[b_0^\dagger] \rho \quad (11)$$

using the time-independent operators b_0, b_0^\dagger , leading to reasonable description for moderate modulations strengths [20]. The temperature T of the environment thermalizes the oscillator towards a mean vibrational quantum number $\bar{m} = [\exp(\hbar\nu_0/k_{\text{B}}T) - 1]^{-1}$ in the unmodulated case. We have used the short notation $\mathcal{D}[X] \rho = 2X\rho X^\dagger - \{X^\dagger X, \rho\}$ for a Lindblad-form term.

B. Displaced frame

In order to eliminate the pump, we unitarily transform $\rho = U\rho'U^\dagger$ with the help of

$$U = D_a(\alpha(t))D_{b_0}(\beta(t)) \quad (12)$$

consisting of the displacement operators $D_a(\alpha) = \exp[\alpha a^\dagger - \alpha^* a]$ for the cavity and the $D_{b_0}(\beta) = \exp[\beta b_0^\dagger -$

$\beta^*b_0]$ for the mechanical oscillator. In the displaced picture, the master equation reads (primes at ρ omitted)

$$\begin{aligned} \frac{\partial \rho}{\partial t} &= \mathcal{L}\rho \\ &= \frac{1}{i\hbar}[H'_{\text{cav}} + H_{\text{mec}}(t) + H'_{\text{rad}}, \rho] + \mathcal{L}_\kappa\rho + \mathcal{L}_\gamma\rho, \end{aligned} \quad (13)$$

if the parameters $\alpha(t)$ and $\beta(t)$ are chosen such that they fulfill the differential equations

$$\dot{\alpha}(t) = \{i[\delta + 2\chi_0\text{Re}\beta(t)] - \kappa\} \alpha(t) - i\frac{\Omega}{2}, \quad (14a)$$

$$\dot{\beta}(t) = -\left\{\frac{\gamma(t)}{2} + i\nu_+(t)\right\} \beta(t) + i\beta^*\nu_-(t) + i\chi_0|\alpha(t)|^2, \quad (14b)$$

together with their complex conjugated counterparts and $\nu_\pm(t) = [\nu_0 \pm \nu^2(t)/\nu_0]/2$. Then, the transformed Hamiltonians take on the form

$$H'_{\text{cav}} = -\hbar\delta'(t)a^\dagger a \quad (15)$$

$$H'_{\text{rad}} = -\hbar\chi_0 [a^\dagger a + \alpha(t)a^\dagger + \alpha^*(t)a] (b_0 + b_0^\dagger) \quad (16)$$

with $\delta' = \delta + 2\chi_0\text{Re}\beta(t)$. We assume that the cavity is strongly driven, such that $|\alpha| \gg 1$, boosting in that way the linear optomechanical coupling.

C. Linearized interaction

If the cavity is sufficiently strongly pumped, the mean field α becomes much larger than the field fluctuations and the term proportional to $a^\dagger a$ in the interaction Hamiltonian (16) can be omitted [21]. The master equation (13) can then be brought into a quadratic form [22]

$$\frac{\partial \rho}{\partial t} = \frac{1}{i\hbar} \left[\vec{R}^T \hat{H} \vec{R}, \rho \right] + \sum_{k=1}^3 \frac{\gamma_k}{2} \mathcal{D} \left[\vec{L}_k \vec{R} \right] \rho, \quad (17)$$

where the vector operator $\vec{R} = (x_c, p_c, x_m, p_m)^T$ contains the dimensionless position and momentum operators $x_m = (b_0 + b_0^\dagger)/\sqrt{2}$ and $p_m = (b_0 - b_0^\dagger)/\sqrt{2}i$ and the corresponding expression for x_c, p_c associated with the cavity field mode. The expectation values of position and momentum and the covariances of the state ρ are contained in the expressions

$$\vec{r} = \langle \vec{R} \rangle \quad (18)$$

$$(\hat{C})_{ij} = \frac{1}{2} \langle R_i R_j + R_j R_i \rangle - \langle R_i \rangle \langle R_j \rangle. \quad (19)$$

They fulfill the dynamical equations

$$\frac{\partial}{\partial t} \vec{r}(t) = \hat{H}_{\text{eff}} \vec{r}(t), \quad (20)$$

$$\frac{\partial}{\partial t} \hat{C}(t) = \hat{H}_{\text{eff}} \hat{C}(t) + \hat{C}(t) \hat{H}_{\text{eff}}^T + \hat{J} \quad (21)$$

following from Eq. (17). Here, $\hat{H}_{\text{eff}} = 2\hat{\sigma}[\hat{H} + \text{Im}\hat{\Gamma}]$ and $\hat{J} = 2\hat{\sigma}[\text{Re}\hat{\Gamma}]\hat{\sigma}^T$, whereby the matrix $\hat{\Gamma}$ incorporates the dissipative dynamics and is defined in terms of the quantities \vec{L}_k in App. A. Moreover, we introduced the symplectic form $\hat{\sigma}_{ij} = [R_i, R_j]/i$. Equations (20) and (21) together with the solution of Eq. (14) are used for a numerical propagation of an initial thermal (Gaussian) state with mean vibrational number \bar{m} towards the quasi-stationary solution in a stable parameter regime. The mean phonon number

$$\langle m \rangle(t) = \frac{1}{2} [C_{33}(t) + C_{44}(t) - 1]. \quad (22)$$

can then be extracted from the propagated covariance matrix \hat{C} .

III. COOLING THE MECHANICAL MOTION

In this section we study the cooling of the mechanical object with modulated frequency and damping in different parameter regimes. Throughout this work we consider a weak optomechanical interaction, such that $|\alpha|\chi_0/\nu \ll 1$. Cooling and heating is then achieved by light scattering at the cavity into the Anti-Stokes and Stokes components, which are associated with the annihilation and creation of a single vibrational quantum. If the cooling rate A_- , *i.e.* the rate of Anti-Stokes scattering is larger than the heating rate A_+ belonging to Stokes scattered light, the mechanical oscillator converges to the stationary state of laser cooling. In the following we develop a theoretical description of the stationary state of cooling for a modulated oscillator.

A. Perturbation theory and adiabatic approximation

In order to get insight into the dynamics when the mechanical element's properties periodically depend on time, we derive an effective master equation for the determination of the stationary state. The applied procedure relies on the weak mechanical coupling, expressed by $\eta = |\alpha|\chi_0/\nu \ll 1$. As a consequence, the dynamics splits into a hierarchy of time scales [21]: A fast time scale given by the free evolution of cavity and oscillator, and a slower time scale on which the optomechanical interaction takes place. The time scale of the modulation we also assume here to be fast, *i.e.* of the order of the mechanical frequency ν . We expand the Liouvillian \mathcal{L} from Eq. (13) according to

$$\mathcal{L} = \mathcal{L}_0 + \mathcal{L}_1. \quad (23)$$

into different orders in the small parameter χ_0/ν with

$$\begin{aligned} \mathcal{L}_0(t)\rho &= \mathcal{L}_c + \mathcal{L}_m(t) \\ &= \left(\frac{1}{i\hbar} [H_{\text{cav}}, \rho] + \mathcal{L}_\kappa \rho \right) + \frac{1}{i\hbar} [H_{\text{mec}}(t), \rho], \end{aligned} \quad (24)$$

$$\mathcal{L}_1 \rho = \frac{1}{i\hbar} [H'_{\text{rad}}, \rho], \quad (25)$$

where we neglected the small correction of the cavity detuning and omitted the damping of the high- Q oscillator momentarily.

In lowest order in η , the optical and mechanical degree of freedom are decoupled, *i.e.* both degrees of freedom evolve independently. The Liouvillian depends explicitly on time due to the modulation of the mechanical frequency. In App. B 1 we introduce its spectral decomposition

$$\mathcal{L}_0(t) = \sum_\lambda \lambda(t) \mathcal{P}_0^\lambda (b_0, b_0^\dagger), \quad (26)$$

with the eigenvalues

$$\lambda_0(t) = \lambda_c + \lambda_m(t) \quad (27)$$

being a sum of the eigenvalues of \mathcal{L}_c and \mathcal{L}_m , whereby $\lambda_m(t) = ik\nu(t)$ with integer k . In Eq. (26) we neglected the time-dependency of the projectors \mathcal{P}_0^λ and use the projectors of the unmodulated oscillator: This is an adiabatic approximation being valid as long as transitions between subspaces belonging to different λ can be neglected during the time evolution. One can estimate the condition $(\langle m \rangle + 1) \frac{\nu}{4\nu^2} \ll 1$ for this approximation to be valid by considering the overlap between energy eigenstates and their derivative with respect to time.

In lowest order of perturbation theory, all projectors on mechanical energy eigenstates are quasi-stationary states, since their eigenvalues λ_m vanish. In higher order in the optomechanical interaction, this degeneracy is lifted, thereby singling out the unique asymptotic state of laser cooling.

The cavity and oscillator degrees of freedom are coupled in first order by the Liouvillian \mathcal{L}_1 . In \mathcal{L}_1 we can replace $\alpha(t)$ with the solution of Eqs. (14) in lowest order in χ_0/ν , which is the constant [23],

$$\alpha_0 = \frac{\Omega/2}{\delta + i\kappa}. \quad (28)$$

Using the annihilation and creation operators of the unmodulated oscillator, b and b^\dagger , the interaction term of the Liouvillian reads

$$\mathcal{L}_1 = \frac{1}{i\hbar} [Fx, \rho]. \quad (29)$$

In the last step we defined the operator

$$F = -\hbar g [a^\dagger a + \alpha_0 a^\dagger + \alpha_0^* a]. \quad (30)$$

acting on cavity states only. The further calculations follow the standard theory of optomechanical laser cooling [21] and is summarized in App. B 2.

To proceed, we consider the slowly evolving subspace belonging to the eigenvalue $\lambda = 0$, whose degeneracy is lifted in second order perturbation theory, hence determining the unique final state of laser cooling. The dynamics in this subspace selected by $\mathcal{P} = \mathcal{P}_0^{\lambda=0}$ is governed by the master equation

$$\mathcal{P}\dot{\rho}(t) = \sum_{\lambda \neq 0} \mathcal{P}\mathcal{L}_1 \mathcal{K}_\lambda(t) \mathcal{L}_1 \mathcal{P}\rho(t), \quad (31)$$

with the superoperator

$$\mathcal{K}_\lambda(t) = \int_0^\infty d\tau e^{\lambda_c \tau} \left\{ e^{t-\tau} \int dt' \lambda_m(t') \right\} \mathcal{P}_0^\lambda. \quad (32)$$

In the following we evaluate the latter expression for specific modulations of the mechanical frequency.

B. Periodic modulations

We assume that the frequency of the mechanical oscillator $\nu(t)$ is changed periodically in time, that is

$$\nu(t) = \nu_0 + f(t) \quad (33)$$

with a real-valued periodic function $f(t+T) = f(t) = \sum_{l=-\infty}^{\infty} c_l e^{il\omega t}$, whereby $\omega = 2\pi/T$. We further assume that the time averaged function $\langle f(t) \rangle_t = 0$ vanishes. This can always be achieved if a non-vanishing mean value is incorporated into ν_0 . Then, the term in the curly brackets in Eq. (32) is also periodic in t with period T , and can be represented as a Fourier series $\sum_\ell K_\ell^{\lambda_m}(t) \exp[i\ell\omega t]$. After performing the τ -integral, one finds

$$\mathcal{K}_\lambda(t) = \sum_\ell K_\ell^{\lambda_m}(t) \frac{-\mathcal{P}_0^\lambda}{\lambda_c + \lambda_m + i\ell\omega}. \quad (34)$$

The evaluation of Eq. (31) using the form (34) again goes along the lines of laser cooling theory and is reported in App. B 3. The resulting master equation of cooling contains the heating and cooling rates

$$A_\pm = \sum_\ell \langle K_\ell \rangle_t \frac{2\kappa\chi_0^2 |\alpha_0|^2}{(\delta \mp [\nu_0 + \ell\omega])^2 + \kappa^2}, \quad (35)$$

which are already time-averaged over one period T with

$$\langle K_l \rangle_t = \left(\frac{1}{2\pi} \right)^2 \left| \int_0^{2\pi} e^{-il\tau} \exp \left[\sum_m \frac{c_m}{m\omega} e^{im\tau} \right] d\tau \right|^2. \quad (36)$$

The time averaging is justified when the modulation frequency belongs to the fast time scales of \mathcal{L}_0 , but still is

slow enough to fulfill the adiabaticity condition. Equation (35) is the central result of this work. The rates of heating and cooling considered as a function of δ are a superposition of Lorentzians, centered at $\pm(\nu + \ell\omega)$ and weighted by the time-averaged Fourier-coefficients $\langle K_l \rangle_t$. In the resolved sideband-limit where $\kappa \ll \nu, \omega$, the Lorentzians are resolved and lead to several resonances in the cooling and heating of the mechanical element. In the case of sinusoidal modulation,

$$f(t) = \hat{\nu} \sin(\omega t) \quad (37)$$

the coefficients $K_l^{\lambda_m}(t)$ are up to a time-dependent phase given by Bessel functions

$$K_l^{\lambda_m}(t) = e^{-i\frac{k\hat{\nu}}{\omega} \cos \omega t} e^{-il\omega t} i^l J_l(k\hat{\nu}/\omega) \quad (38)$$

of order l with the index k determining the mechanical eigenvalue $\lambda_m = ik\nu_0$ of the unmodulated oscillator. Time averaging leads to

$$\langle K_l \rangle_t = J_l(\hat{\nu}/\omega)^2 \quad (39)$$

in the rates A_{\pm} .

Fig. 2 illustrates the dependency of the rates A_{\pm} , Eq. (35), on the detuning Δ (colored curves). Moreover, the rates before time-averaging, using Eq. (38), for a sinusoidal modulation (black curves) are shown. In a) a fast modulation $\omega = \nu/2$ was chosen. The time-dependent curves show rapid oscillations of sideband peaks that even can become negative. The cooling dynamics can not follow these rapid oscillations, but after time-averaging positive sidebands at $\pm\omega$ around the main resonances at $\pm\nu$ survive, which influence the final state of laser cooling. On the contrary, for slow modulations $\omega = 0.01\nu$ presented in b), the sidebands overlap and lead to a periodically moving, positive resonance. In the resolved sideband-limit $\kappa \ll \nu$, the optimal detuning is given by the maximum of A_- , which sweeps through different values of Δ .

C. Stationary state

The time-averaged stationary state of the mirror's motion we calculate from the rates (35) giving

$$\mu_{st} = \left(1 - \frac{A_-}{A_+}\right) \left(\frac{A_-}{A_+}\right)^{b_0^\dagger b_0} \quad (40)$$

with mean vibrational occupation number

$$\langle m \rangle = \text{Tr}[b_0^\dagger b_0 \mu_{st}] = \frac{A_+}{A_- - A_+}, \quad (41)$$

which corresponds to the temperature at the end of the cooling procedure. The average cooling rate is given by

$$\Gamma = A_- - A_+. \quad (42)$$

and estimates the time scale on which the stationary state is reached.

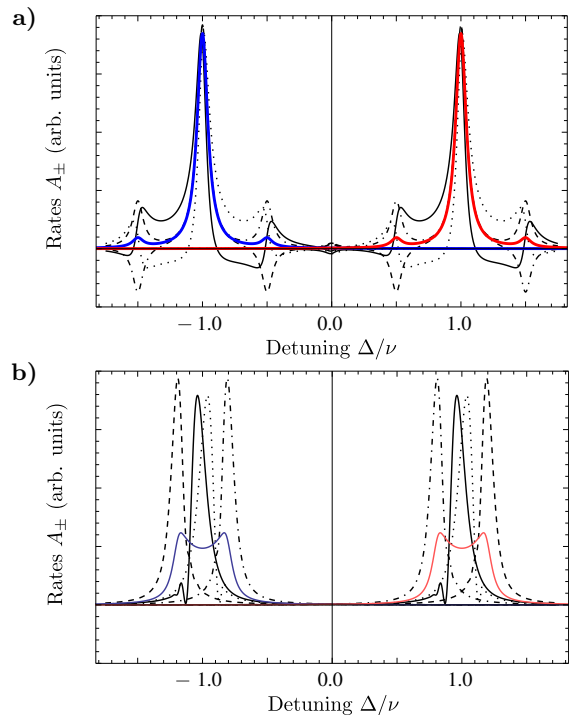


FIG. 2. The rates A_{\pm} for a sinusoidal modulation. The blue (red) line represents the time average A_- (A_+), Eq. (35). The black curves show the same rates before averaging at different times $t = 0, T/4, T/2$ and $3T/4$ of a modulation period. In a) the fast modulation $\omega = \nu/2$ generates rapidly oscillating sidebands displaced by multiples of ω from the main resonance at $\Delta = \pm\nu$. The sidebands have a non-vanishing temporal mean as shown by the colored curves. Slow modulations with $\omega = \nu/100$, in b), essentially move the resonance peaks along the momentary oscillator frequency. Other parameters are $\hat{\nu} = 0.2\nu$, $\kappa = 0.05\nu$.

In Fig. 3 we show the mean vibrational occupation number $\langle m \rangle$, Eq. (41), at the end of the cooling procedure (curve) and compare it with numerical solutions (dots) obtained from Eq. (22). Low phonon numbers are found whenever the detuning coincides with a resonance of A_- in this resolved sideband limit. Small deviations are found at the sideband minima which we attribute to the adiabatic approximation performed in the theory. In the inset, the numerically calculated time dependency of the mean phonon number, starting from an initial state with $\langle m \rangle(t=0) = 3$, is shown for different detunings. The decay rate of the curve corresponds to Γ , Eq.(42), and one finds indeed that the stationary state is approached faster close to a cooling resonance, where A_- has a maximum.

Up to this point, the presented treatment ignored the thermalization of the mechanical oscillator due to coupling to its environment, which takes place with the rate γ . For high-Q oscillators, γ can be considered as the slowest time scale involved in the dynamics. If this is the

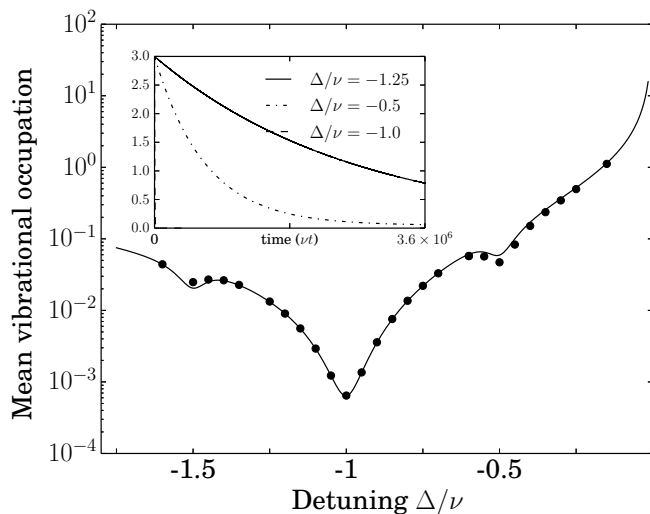


FIG. 3. Comparison between the analytic approximation, Eq. (41), (solid line) and numerical results (points) for sinusoidal modulation. In the inset, the numerically calculated time curve $\langle m \rangle(t)$ is shown for selected values of Δ . Parameters are $\hat{\nu} = 0.1\nu$, $\kappa = 0.05\nu$, $\omega = \nu/2$, $\gamma = 0$, $\bar{m} = 0$.

case, the final vibrational occupation number results as

$$\overline{\langle m \rangle} = \frac{\langle m \rangle \Gamma_{\text{cool}} + \bar{m} \gamma}{\Gamma_{\text{cool}} + \gamma}. \quad (43)$$

In the adiabatic limit, $\Gamma_{\text{cool}} = \Gamma$, Eq. (42) can be calculated directly from A_{\pm} .

If the damping rate becomes comparable to the cooling rate, the damping should be incorporated into \mathcal{L}_1 , but, since \mathcal{L}_γ does not couple the \mathcal{P} and $1 - \mathcal{P}$ subspaces, the theory predicts no interplay between damping and optomechanical interactions. For even stronger damping, apart of the fact that the description in Eq. (11) becomes questionable, the laser cooling would take place on a much slower time scale, meaning that the mechanical element would take on a stationary state close the thermal state.

D. Influence of pulse shape

The strength of the sidebands in the rates A_{\pm} , Eq. (35), is determined by the coefficients $\langle K_l \rangle$ which in turn depend on the Fourier coefficients c_m of the pulse $f(t)$ and can therefore be manipulated by altering the pulse form. By modifying the modulation parameters or using higher harmonics in $f(t)$ it is hence possible to shape the resonances of A_{\pm} . However, suppressing resonances in the heating rate A_+ for efficient cooling can not be achieved, since all $\langle K_l \rangle_t$ are non-negative.

Fig. 4 shows an example using the first ten Fourier coefficients of a rectangular shaped pulse, leading to a $f(t)$ as shown in inset a). The modulation frequency is chosen here to be smaller, $\omega = \nu/6$ such that with

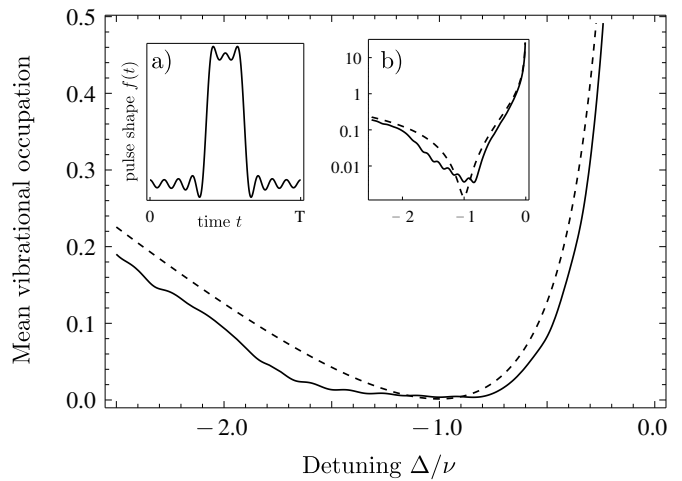


FIG. 4. Mean phonon number $\langle m \rangle$, Eq. (41), for a pulse $f(t)$, shown in inset a), comprising several harmonics. It is compared to the unmodulated case (dashed curve). In inset b) a logarithmic plot shows that the modulation increases the minimal achievable temperature. The parameters are $\hat{\nu} = 0.5\nu$, $\kappa = 0.07\nu$, $\gamma = 0$, $\bar{m} = 0$, $\omega = \nu/6$.

$\kappa = 0.07\nu$ adjacent resonances in the rates A_{\pm} start to overlap. In this way it is possible to broaden the cooling resonance and forming a plateau-like behavior of $\langle m \rangle(\Delta)$ around the lowest temperature. This can be achieved on the cost of an increased minimal temperature as the curves in the logarithmic scale of inset b) clearly shows.

IV. NUMERICAL RESULTS AND DISCUSSION

In order to extend the analysis beyond the theoretical treatment, we proceed with a numerical simulation of the optomechanical dynamics. We will analyze a large parameter regime of modulation frequencies and incorporate the damping of the mechanical element.

For the treatment discussed here, we focus again on a sinusoidal modulation

$$\nu(t) = \nu_0 + \hat{\nu} \sin(\omega t), \quad (44)$$

$$\gamma(t) = \gamma_0 + \hat{\gamma} \sin(\omega t), \quad (45)$$

and first solve numerically the coupled differential equations (14). By means of the behavior of the mean values $\alpha(t)$ and $\beta(t)$ we are able to exclude parameter regimes showing optomechanical instability [24] or where the system becomes unstable due to parametric amplification, as it is found at the resonances $\omega = \nu$ and especially around $\omega = 2\nu$. The time-dependent mean values are used in the linearized equation (21) in order to calculate the time-averaged value of the mean vibrational occupation number $\langle m \rangle$ in the quasi-stationary, oscillatory regime at the final stage of the cooling. We also extract the cooling rate from the numerical data by fitting an exponential decay to $\langle m \rangle(t)$, calculated from Eq. (22). For the rest of this section we investigate the behavior of $\langle m \rangle$

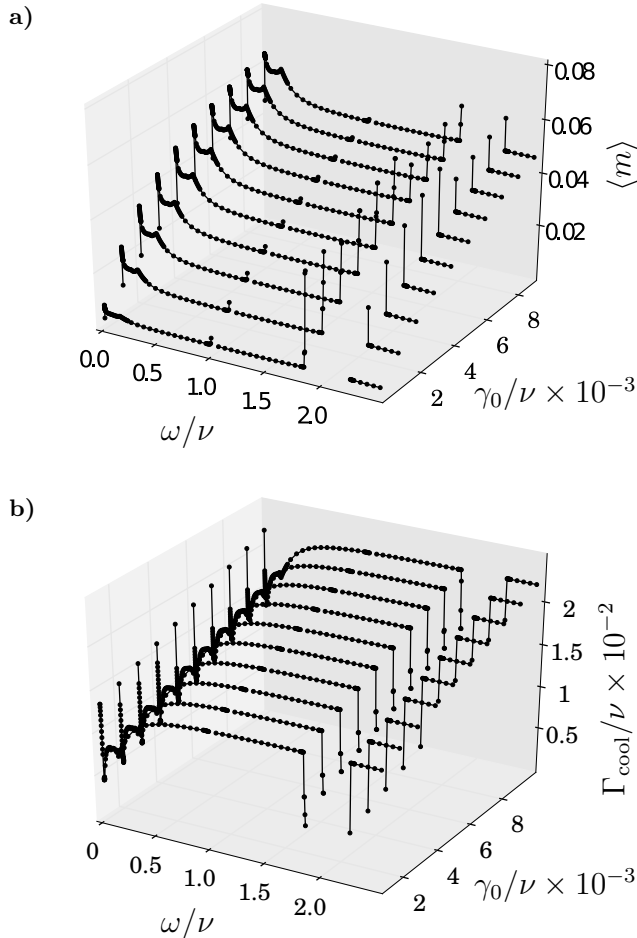


FIG. 5. **a)** Mean vibrational occupations number as a function of the modulation frequency ω and damping γ . For each point, the detuning was optimized in order to find the minimal occupation number. Missing lines between the points mark regions where the system is unstable. **b)** Same as in **a)** but showing the cooling rate Γ_{cool} . Parameters: $\hat{\nu} = 0.2\nu$, $\hat{\gamma} = 0.2\gamma_0$, $\kappa = 0.1\nu$ and $\eta = 0.25$ at resonance.

and Γ_{cool} for a wide range of modulation frequencies and dampings γ_0 . The results are depicted in Fig. 5a) where we show the minimal value of the time-averaged occupation number $\langle m \rangle$ after scanning through the detuning Δ , as a function of ω and γ_0 in the quasi-stationary regime.

For ω in the vicinity of zero, the vibrational occupation number increases rapidly as ω increases. The change in the oscillator frequency makes it impossible for the external field to stay tuned to the optimal cooling frequency when $\kappa \ll \nu$, explaining the sudden drop-off. This can be compared to the case depicted in Fig. 2b): The oscillatory moving resonance curve (black lines) sweeps through the constant laser frequency such that a fixed resonance condition is lost. When the modulation frequency ω becomes larger, the time averaged resonance curve, *i.e.* the colored curve in Fig. 2b), becomes relevant and the temperature decreases again, until it stays for a small range of modula-

tion frequency on a plateau-like level with hardly visible small resonances, terminated by a final distinct resonance peak at $\omega \approx 0.15\nu$. Similar to the smaller peaks, the final peak can be explained by the zeros of the Bessel functions in the time-averaged rates A_{\pm} , Eqs. (35) and (39). This becomes clear when recalling that the rates A_{\pm} can be decomposed into Lorentzian peaks with intensity proportional to $J_l(\hat{\nu}/\omega)$, with $l = 0$ marking the central peak. For growing ω the argument of the Bessel function decreases and from a certain modulation frequency on, the Bessel function passed through its last zero and monotonically increases afterwards. This modulation frequency marks the point from which on the strength of the central peak only grows. When it overtops the lateral peaks it uniquely defines the lowest temperature and this is the point, where the final maximum of the plateau-like structure in Fig. 5a) is situated. From here on, the optimal detuning for lowest temperature is $\Delta = \nu$ and the temperature falls off for larger values of ω . Not before $\omega = \nu$, another increase of the temperature can be observed in the figure, due to a resonance with the vibrational frequency. At $\omega = 2\nu$ a strong increase of the temperature occurs. This is the parameter regime discussed in detail in Ref. [16], where also squeezing of the oscillator's state and increased entanglement between the optical and mechanical degree of freedom emerges. The increase in temperature can qualitatively also be understood from the rates A_{\pm} : Then, the first red sideband of the rate of heating A_+ coincides with the central peak of the rate of cooling A_- .

Within the parameter range used here, no significant influence stemming from the modulation of $\gamma(t)$ was found that could not be reproduced by replacing $\gamma(t)$ with its average value γ_0 for all considered time-averaged observables. The dependency of $\langle m \rangle$ on γ_0 mainly leads to an overall increase of the vibrational occupation due to the stronger coupling to the environmental heat bath. Apart from it, the course of $\langle m \rangle$ for small ω shows a much stronger initial increase of the temperature and the plateau-like behavior is intensified, especially for mid-level values of γ_0 . Also a counterbalancing of the fluctuation of $\langle m \rangle$ around the resonance at $\omega = \nu$ can be observed. Apart from these details, one has to conclude that the damping of the modulated oscillator does not show beneficial effects for cooling, but behaves as expected from a stronger coupling to the heat bath.

In Fig. 5b) we plot the cooling rate Γ_{cool} as a function of ω and γ_0 . It shows an overall reciprocal behavior compared to the final temperature shown in 5b), as Eq. (42) suggests. The cooling rate increases almost linearly with larger γ , without changing significantly the shape with respect to ω . For very small modulations, the cooling rate falls off strongly. Moreover, the resonance at $\omega = \nu$ is hardly visible, but at $\omega = 2\nu$ we find again that efficient cooling breaks down in favor of increased non-classical properties of the optomechanical system.

We finally remark that for larger values of κ the fine structure of the curves in Fig. 5 are washed out due to

the stronger overlapping sidebands in A_{\pm} .

V. CONCLUSIONS

We studied in detail the effect of laser cooling when the frequency of the harmonically supported mechanical element $\nu(t)$ and its dissipation rate $\gamma(t)$ depend on time. We obtained analytic approximations valid in the adiabatic limit when $\dot{\nu}(t)/\nu^2 \ll 1$. When $\omega \approx \nu$ or larger and when the setup is in the resolved sideband regime, several cooling resonances can be found, whose relative strength depend on the pulse shape. The form of the periodic modulation pulses allows to shape the cooling resonances as a function of the laser frequency to a certain extent. With the help of simple expressions for the time-averaged rates of heating and cooling, a physical picture for the temporal behavior of the cooling process could be provided.

We complemented the analysis of cooling a modulated optomechanical setup by numerical investigations covering a larger range of parameters, whose results generally confirm the analytic predictions. At least qualitatively, the insight provided by the theoretical model allows to explain most of the numerical findings. Moreover, we found that the time dependency of $\gamma(t)$ does not alter qualitatively neither the final temperature nor the decay rates of the cooling process. If the interest is only in the time-averaged behavior, the modulation of the damping can even be ignored. The analysis of this work provides a deeper insight into the cooling dynamics when the properties of the mechanical oscillator are modulated and can serve as a guidance for current experiments when the temporal behavior of the mechanical element are controllable in time.

ACKNOWLEDGMENTS

We thank Phillipp Treutlein and Andreas Jöckel for drawing our attention on this topic. Moreover, we are thankful to Luis Octavio Castaños for many helpful discussions. This work was supported by project PAPIIT IN103714 and was triggered during the the Kolleg ‘‘Open quantum systems: Chaos and decoherence’’ at the Centro Internacional de Ciencias, Cuernavaca, Mexico, funded by the Alexander-von-Humboldt foundation.

Appendix A: Elements of the linearized master equations

The explicit forms of the matrices and vectors appearing in Eqs. (17) follow directly from the master equation (13) in the linearized form, *i.e.*, after omitting the term proportional to $a^\dagger a$ in the optomechanical interac-

tion. One finds

$$\hat{H} = \hbar \begin{pmatrix} -\frac{\Delta}{2} & 0 & -\frac{\chi_0}{2}(\alpha + \alpha^*) & 0 \\ 0 & -\frac{\Delta}{2} & -\frac{i\chi_0}{2}(\alpha^* - \alpha) & 0 \\ -\frac{\chi_0}{2}(\alpha + \alpha^*) & -\frac{i\chi_0}{2}(\alpha^* - \alpha) & \frac{\nu}{2} & 0 \\ 0 & 0 & 0 & \frac{\nu}{2} \end{pmatrix} \quad (\text{A1})$$

and for the jump vectors

$$\vec{L}_1 = \frac{1}{\sqrt{2}} \begin{pmatrix} 1 \\ i \\ 0 \\ 0 \end{pmatrix}, \quad \vec{L}_2 = \frac{1}{\sqrt{2}} \begin{pmatrix} 0 \\ 0 \\ 1 \\ i \end{pmatrix}, \quad \vec{L}_3 = \frac{1}{\sqrt{2}} \begin{pmatrix} 0 \\ 0 \\ 1 \\ -i \end{pmatrix}. \quad (\text{A2})$$

Furthermore, we defined

$$\gamma_1 = 2\kappa, \quad \gamma_2 = \gamma(\bar{m} + 1), \quad \gamma_3 = \gamma\bar{m}. \quad (\text{A3})$$

The matrix $(\hat{\Gamma})_{mn} = \sum_k \gamma_k (\vec{L}_k)_m^* (\vec{L}_k)_n$ is needed for the time evolution, Eq. (21), of the covariance matrix \hat{C} . It has the explicit form

$$\Gamma = \frac{1}{2} \begin{pmatrix} \kappa & i\kappa & 0 & 0 \\ -i\kappa & \kappa & 0 & 0 \\ 0 & 0 & \frac{\gamma}{2}(2\bar{m} + 1) & \frac{i}{2}\gamma \\ 0 & 0 & -\frac{i}{2}\gamma & \frac{\gamma}{2}(2\bar{m} + 1) \end{pmatrix}. \quad (\text{A4})$$

With these quantities the time evolution of Gaussian states can be written in the compact notation given in Sec. II C.

Appendix B: Derivation of effective master equation

1. Spectral decomposition of \mathcal{L}_0

In this section we discuss the eigensystem of $\mathcal{L}_0 = \mathcal{L}_c + \mathcal{L}_m(t)$, Eq. (25). To this end we introduce the eigenelements $\hat{\rho}^\lambda(t)$ and $\check{\rho}^\lambda(t)$ which are elements of the operator space and fulfill instantenous the eigenvalue equations

$$\mathcal{L}_0(t)\hat{\rho}^\lambda(t) = \lambda(t)\hat{\rho}^\lambda(t) \quad (\text{B1})$$

$$\check{\rho}^{\lambda\dagger}\mathcal{L}_0(t) = \lambda(t)\check{\rho}^{\lambda\dagger}(t). \quad (\text{B2})$$

These eigenelements are orthogonal $\text{Tr}\{(\check{\rho}^\lambda)^\dagger \hat{\rho}^{\lambda'}\} = \delta_{\lambda,\lambda'}$ with respect to the scalar product $(A, B) = \text{Tr}[A^\dagger B]$. The projectors $\mathcal{P}_0^\lambda = \check{\rho}^\lambda \otimes \hat{\rho}^\lambda$ project an arbitrary operator X onto the subspace belonging to λ according to $\mathcal{P}_0^\lambda X = \hat{\rho}^\lambda \text{Tr}[\check{\rho}^{\lambda\dagger} X]$. If the eigensystem of \mathcal{L}_0 is complete, the projectors fulfill

$$\sum_\lambda \mathcal{P}_0^\lambda = 1. \quad (\text{B3})$$

Since in lowest order perturbation theory \mathcal{L}_0 is a sum of the cavity and mechanical part without interaction, the

eigensystem can be decomposed into

$$\hat{\rho}^\lambda(t) = \hat{\rho}_c^\lambda \hat{\rho}_m^\lambda(t), \quad \check{\rho}^{\lambda\dagger}(t) = \hat{\rho}_c^{\lambda\dagger} \hat{\rho}_m^{\lambda\dagger}(t), \quad (\text{B4})$$

$$\mathcal{P}_0^\lambda(t) = \mathcal{P}_c^\lambda \mathcal{P}_m^\lambda(t). \quad (\text{B5})$$

and

$$\lambda_0(t) = \lambda_c + \lambda_m(t). \quad (\text{B6})$$

The explicit form of the cavity eigenelements can be found in Ref. [25] with the corresponding eigenvalues

$$\lambda_c(k, n) = ik\Delta - (2n + |k|)\kappa, \quad (\text{B7})$$

where k are integers and n non-negative integers. The mechanical eigenelements can be constructed from the instantaneous eigenstates $|m(t)\rangle$ of $H_{\text{mec}}(t)$ and have the simple form

$$\hat{\rho}_m^\lambda(t; n, l) = \begin{cases} |n\rangle\langle n+l| & l \geq 0 \\ |n+|l\rangle\langle n| & l < 0 \end{cases} \quad (\text{B8})$$

with $\lambda_m(t; n, l) = i\nu(t)$ and $\check{\rho}_m^{\lambda m} = \hat{\rho}_m^{\lambda m}$. These eigenelements are infinitely degenerate in the index n .

2. Effective master equation of cooling

We start with the Liouvillian from Eq. (23) and define the time-independent projectors

$$\mathcal{P} = \mathcal{P}_c^{\lambda_c=0} \mathcal{P}_m^{\lambda_m=0} \quad (\text{B9})$$

$$\mathcal{Q} = 1 - \mathcal{P} \quad (\text{B10})$$

in the adiabatic approximation discussed in the main text. The goal is to find an effective master equation in the subspace selected by \mathcal{P} valid up to second order in the parameter η characterizing the optomechanical coupling strength. We project the master equation $\dot{\rho} = \mathcal{L}\rho$ onto the subspaces belonging to \mathcal{P} and \mathcal{Q} , insert $1 = \mathcal{P} + \mathcal{Q}$, and use the expansion (23) of \mathcal{L} , yielding

$$\mathcal{P}\dot{\rho}(t) = \mathcal{P}\mathcal{L}_1\mathcal{Q}\rho(t) \quad (\text{B11})$$

$$\mathcal{Q}\dot{\rho}(t) = \mathcal{Q}\mathcal{L}_1\mathcal{P}\rho(t) + \mathcal{Q}\mathcal{L}_0\mathcal{Q}\rho(t). \quad (\text{B12})$$

In the last step we exploited that $\mathcal{P}\mathcal{L}_0 = \mathcal{L}_0\mathcal{P} = 0$ with the approximated \mathcal{L}_0 from Eq. (26) and that \mathcal{L}_1 does not couple states in \mathcal{P} , hence $\mathcal{P}\mathcal{L}_1\mathcal{P} = 0$. Moreover, we neglected \mathcal{L}_1 in the last term of the second equation, since it would lead to higher order correction. The second

equation can be formally integrated leading to

$$\begin{aligned} \mathcal{Q}\rho(t) = & e^{\int_{t_0}^t dt' \mathcal{Q}\mathcal{L}_0(t')} \mathcal{Q}\rho(t_0) \\ & + e^{\int_{t_0}^t dt' \mathcal{Q}\mathcal{L}_0(t')} \int_{t_0}^t dt' e^{-\int_{t_0}^{t'} dt'' \mathcal{Q}\mathcal{L}_0(t'')} \mathcal{Q}\mathcal{L}_1\mathcal{P}\rho(t'). \end{aligned} \quad (\text{B13})$$

The integration interval $\Delta t = t - t_0$ is assumed here to be large for the fast time scale of zeroth order and short for the time scale of interaction: The first term thus dies off rapidly whereas in the second term one can replace $\mathcal{P}\rho(t')$ by $\mathcal{P}\rho(t)$. Plugging this result into Eq. (B11) and inserting the completeness relation $\sum_\lambda \mathcal{P}^\lambda = 1$ yields the closed master equation of the main text, Eq. (31), where we further used Eq. (B6) and set $\Delta t \rightarrow \infty$ in the limits of the τ -integral.

3. Cooling and heating rates

Inserting Eq. (34) into the effective master equation (31) and tracing over the cavity degrees of freedom yields

$$\dot{\mu} = \sum_{\lambda \neq 0} \sum_l \frac{K_l^{\lambda m}}{\lambda_c + \lambda_m + i\ell\omega} \text{Tr}_c \{ \mathcal{P}\mathcal{L}_1\mathcal{P}_0^\lambda \mathcal{L}_1 \varrho_c \mu \} \quad (\text{B14})$$

with the density operator $\mu = \text{Tr}_c \mathcal{P}\rho$ and the stationary state $\varrho_c = |0\rangle\langle 0|$ of the cavity, full filling $\mathcal{L}_c \varrho_c = 0$. The coefficients fulfill $K_l^{\lambda m}(t) = K_{-l}^{-\lambda m*}(t)$. The trace is calculated using Eq. (29), and after separating operators belonging to the oscillator and cavity degrees of freedom, the trace term reads

$$\text{Tr}_c \{ \dots \} = T_1(\lambda_c) \mathcal{P}_m^0[x, \mathcal{P}_m^{\lambda_m} x \mu] - T_2(\lambda_c) \mathcal{P}_m^0[x, \mathcal{P}_m^{\lambda_m} \mu x], \quad (\text{B15})$$

whereby

$$T_1(\lambda_c) = \text{Tr}_c \{ F \mathcal{P}_c^{\lambda_c} F \varrho_{\text{st}} \} = \hbar^2 g^2 |\alpha_0|^2 \delta_{\lambda_c, i\delta - \kappa}, \quad (\text{B16})$$

$$T_2(\lambda_c) = \text{Tr}_c \{ F \mathcal{P}_c^{\lambda_c} \varrho_{\text{st}} F \} = \hbar^2 g^2 |\alpha_0|^2 \delta_{\lambda_c, -i\delta - \kappa}. \quad (\text{B17})$$

The mechanical expressions

$$\begin{aligned} \mathcal{P}_m^0[x, \mathcal{P}_m^{\lambda_m} x \mu] = & \xi_0^2 \left\{ (b_0 b_0^\dagger - b_0^\dagger \mu b_0) \delta_{\lambda_m, -i\nu} \right. \\ & \left. + (b_0^\dagger b_0 \mu - b_0 \mu b_0^\dagger) \delta_{\lambda_m, i\nu} \right\}, \end{aligned} \quad (\text{B18})$$

$$\begin{aligned} \mathcal{P}_m^0[x, \mathcal{P}_m^{\lambda_m} \mu x] = & \xi_0^2 \left\{ (b_0 \mu b_0^\dagger - \mu b_0^\dagger b_0) \delta_{\lambda_m, -i\nu} \right. \\ & \left. + (b_0^\dagger \mu b_0 - \mu b_0 b_0^\dagger) \delta_{\lambda_m, i\nu} \right\} \end{aligned} \quad (\text{B19})$$

are calculated with $x = \xi_0(b_0 + b_0^\dagger)$. After plugging Eqs. (B16)–(B19) into Eq. (B14), performing the time averaging with $\langle K_l \rangle_t \equiv \langle K_l^{\lambda_m = i\nu} \rangle = \langle K_{-l}^{\lambda_m = -i\nu} \rangle$, the master equation can be cast into the form

$$\dot{\mu} = \frac{1}{i\hbar} [\tilde{H}, \mu] + \frac{A_-}{2} \mathcal{D}[b_0] \mu + \frac{A_+}{2} \mathcal{D}[b_0^\dagger] \mu \quad (\text{B20})$$

of a damped harmonic oscillator with the rates A_\pm given by Eq. (35) and a small correction $\tilde{H} \propto b_0^\dagger b_0$ to the Hamiltonian of the mechanical oscillator, that is neglected in what follows.

-
- [1] M. Aspelmeyer, T. J. Kippenberg, and F. Marquardt, “Cavity Optomechanics,” (2014), to appear in *Rev. Mod. Phys.*, see also: arXiv:1303.0733 [cond-mat.mes-hall].
- [2] S. Gröblacher, K. Hammerer, M. R. Vanner, and M. Aspelmeyer, *Nature* **460**, 724 (2009).
- [3] E. Verhagen, S. Deleglise, S. Weis, A. Schliesser, and T. J. Kippenberg, *Nature* **482**, 63 (2012).
- [4] M. Eichenfield, J. Chan, R. M. Camacho, K. J. Vahala, and O. Painter, *Nature* **462**, 78 (2009).
- [5] M. Korppi, A. Jöckel, M. T. Rakher, S. Camerer, D. Hunger, T. W. Hänsch, and P. Treutlein, in *European Physical Journal Web of Conferences*, European Physical Journal Web of Conferences, Vol. 57 (2013) p. 3006.
- [6] N. E. Flowers-Jacobs, S. W. Hoch, J. C. Sankey, A. Kashkanova, A. M. Jayich, C. Deutsch, J. Reichel, and J. G. E. Harris, *Appl. Phys. Lett.* **101**, 221109 (2012).
- [7] S. Mancini and P. Tombesi, *Phys. Rev. A* **49**, 4055 (1994).
- [8] I. Wilson-Rae, N. Nooshi, W. Zwerger, and T. J. Kippenberg, *Phys. Rev. Lett.* **99**, 093901 (2007).
- [9] F. Marquardt, J. P. Chen, A. A. Clerk, and S. M. Girvin, *Phys. Rev. Lett.* **99**, 093902 (2007).
- [10] J. Chan, T. P. Mayer Alegre, A. H. Safavi-Naeini, J. T. Hill, A. Krause, S. Gröblacher, M. Aspelmeyer, and O. Painter, *Nature* **478**, 89 (2011).
- [11] J.-Q. Liao and C. K. Law, *Phys. Rev. A* **84**, 053838 (2011).
- [12] S. Machnes, J. Cerrillo, M. Aspelmeyer, W. Wieczorek, M. B. Plenio, and A. Retzker, *Phys. Rev. Lett.* **108**, 153601 (2012).
- [13] Y.-C. Liu, Y.-F. Xiao, X. Luan, and C. W. Wong, *Phys. Rev. Lett.* **110**, 153606 (2013).
- [14] M. R. Vanner, I. Pikovski, G. D. Cole, M. S. Kim, Č. Brukner, K. Hammerer, G. J. Milburn, and M. Aspelmeyer, *Proc. Natl. Acad. Sci. USA* **108**, 16182 (2011).
- [15] A. Mari and J. Eisert, *Phys. Rev. Lett.* **103**, 213603 (2009).
- [16] A. Farace and V. Giovannetti, *Phys. Rev. A* **86**, 013820 (2012).
- [17] A. Jockel, M. T. Rakher, M. Korppi, S. Camerer, D. Hunger, M. Mader, and P. Treutlein, *Appl. Phys. Lett.* **99**, 143109 (2011).
- [18] A. Jayich, J. Sankey, B. Zwickl, C. Yang, J. Thompson, S. Girvin, A. Clerk, F. Marquardt, and J. G. E. Harris, *New J. Phys.* **10**, 095008 (2009).
- [19] M. Wallquist, K. Hammerer, P. Zoller, C. Genes, M. Ludwig, F. Marquardt, P. Treutlein, J. Ye, and H. J. Kimble, *Phys. Rev. A* **81**, 023816 (2010).
- [20] S. Kohler, T. Dittrich, and P. Hänggi, *Phys. Rev. E* **55**, 300 (1997).
- [21] I. Wilson-Rae, N. Nooshi, J. Dobrindt, T. Kippenberg, and W. Zwerger, *New J. Phys.* **10**, 095007 (2008).
- [22] M. Wallquist, K. Hammerer, P. Zoller, C. Genes, M. Ludwig, F. Marquardt, P. Treutlein, J. Ye, and H. Kimble, *Phys. Rev. A* **81**, 023816 (2010).
- [23] Then perturbation theory shows that the first order correction $\alpha_1 = 0$ vanishes, and hence, there is no contribution to \mathcal{L}_2 .
- [24] F. Marquardt, J. G. E. Harris, and S. M. Girvin, *Phys. Rev. Lett.* **96**, 103901 (2006).
- [25] H.-J. Briegel and B.-G. Englert, *Phys. Rev. A* **47**, 3311 (1993).